Journal of Mathematical Modeling
Vol. 8, No. 1, 2020, pp. 41-54

JMM

A macroscopic second order model for air traffic flow

Mahboobeh Hoshyar Sadeghian, Mortaza Gachpazan*, Nooshin Davoodi and Faezeh Toutounian

Department of Applied Mathematics, Faculty of Mathematical Science, Ferdowsi University of Mashhad, Mashhad, Iran

Emails: ma_hs987@mail.um.ac.ir, gachpazan@um.ac.ir, davoodi.math@gmail.com, toutouni@math.um.ac.ir

Abstract. In this paper, we introduce a new dynamic model for the air traffic flow prediction to estimate the traffic distribution for given airspaces in the future. Based on Lighthill-Whitham-Richards traffic flow model and the Newton's second law, we establish a nonlinear model to describe interrelationship and influential factors of the three characteristic parameters as traffic flow, density, and velocity. The upwind scheme is applied to perform the numerical simulations. Numerical results show that the proposed model can reproduce the evolution of shockwave, rarefaction wave, and small perturbation.

Keywords: Air traffic flow, macroscopic model, LWR model, Newton's second law, upwind scheme.
AMS Subject Classification: 35Q35, 35L75, 37M05, 37N30.

1 Introduction

Air traffic flow has been grown during the last decades. Concepts in air traffic flow are basically different from the highway traffic flow. Eulerian models are based on control-volume and conservation equations. The Lagrangian models are trajectory-based and consider the individual aircraft trajectories (see for example [1]). As the number of aircraft has no effect on the dimension of Eulerian models [4], and the errors of the trajectory-based flow prediction increase sharply when

*Corresponding author
Received: 27 November 2019 / Revised: 21 December 2019 / Accepted: 23 December 2019.
DOI: 10.22124/jmm.2019.15035.1359

© 2020 University of Guilan

the forecast time horizon exceeds 20 minutes, Eulerian models have been preferred to Lagrangian ones.

Menon et al. [9] were the first researchers to model air traffic flow using an Eulerian framework. Inspired by their original approach [10] several articles have been presented [2, 3, 11, 12]. Bayen and co-authors [2] derived an Eulerian network model applicable to air traffic flow in the National Airspace System (NAS). In [3] the authors used an Eulerian network model of the airspace to simulate air traffic in congested areas of airspace. Their model relies on a set of coupled first-order hyperbolic PDEs, obtained from the original Lighthill-Whitham-Richards (LWR) traffic flow model. Strub et al. [12] developed a flow model of high altitude traffic in the NAS using an Eulerian description of the network with hyperbolic PDEs. Menon et al. [11] proposed computer-based approaches which are essential for modeling realistic airspaces involving multiple travel streams. They focus on the development of a computer-aided methodology for deriving Eulerian models of the airspace and employing it for air traffic flow control. In [13] Sun and co-authors compared the predictive capabilities of the Large-capacity cell transmission model (CTM(L)) with three other commonly used Eulerian models including the LWR-PDE model [3], the Modified Menon Model (MMM) [9], and the two-Dimensional Menon Model (2DMM) [11]. Ma et al. [8] introduced the Probabilistic Collocation Method (PCM) to provide a simple and efficient numerical solution to LWR-PDE which can save up to %80 of computation time to achieve a solution with the same accuracy. The authors in [4] proposed a dynamic network-based approach for short-term air traffic flow prediction in en-route airspace. In order to study the traffic flow operation on the air freeways, using the car-following theory, Wang et al. [15] established a microscopic plane-following model for a monolayer route with a single direction which is characterized in the next generation aviation transportation system (NGATS). In addition, through the analysis of the relationship between air traffic flow and density, they extended the model to a macroscopic traffic flow model for air freeways.

In this paper, we propose a new macroscopic continuum model for air traffic.

Any flight plan includes origin and destination, a specified airway, the height of the flight, and the speed of flight for different positions of the route. By considering the positions of other planes that are recorded before, if using the flight plan leads to exceeding the flow, it must be changed. Otherwise, it is confirmable.

As in [15], assuming that airplanes fly on a monolayer route with a single direction, a second-order model for air traffic flow is proposed. It is shown that, in this model, the characteristic speeds are not greater than the macroscopic flow velocity.

The rest of this paper is organized as follows. In the following section, the new model is given in the form of microscopic. In Section 3, we obtain the macroscopic form of the proposed model and the stability conditions are investigated. In Section 4, the numerical simulation is presented for some initial and boundary conditions. Finally, some concluding remarks are presented in Section 5.

2 A non-linear air traffic model

As known, the common mathematical model for second-order models in highway traffic flow, is the LWR model, i.e.,

$$\rho_t + f(\rho)_x = 0, \tag{1}$$

where $\rho(x,t)$ denotes the density (the numbers of cars per unit at time t) and $f(\rho)$ is the flux function.

Based on a modified version of LWR model, Bayen et al. in [3], considered the LWR model (1) with $f(\rho) = \rho v$, where $v = v(x)$ is the velocity. In this paper, we assume that v is a function of two variables x and t (i.e., $v = v(x,t)$).

By using Newton's second law (i.e., $F = ma$), and ignoring the angle of engine installation in an aircraft and some other forces (for simplicity), the second equation of the model, is obtained as follows (see Fig. 1.):

$$T_n \cos\alpha - D_n + \beta_1 mg \sin\theta B(\Delta x_n, \Delta v_n) = m\frac{d^2 x_n}{dt^2}, \tag{2}$$

where α is the angle of attack (the angle between the tip of aircraft and the route), θ denotes the angle between the tip of the aircraft and horizontal, $x_n(t)$ is the position of the nth plane at time t, $\Delta x_n = x_{n+1} - x_n$ represents the headway of the nth plane, m denotes the mass of nth plane, g is the acceleration of gravity, D_n represents the drag force, T_n and $B(\Delta x_n, \Delta v_n)$ are respectively the thrust force by the aircraft engine and the brake-control function. We mention that all parameters are considered at time t and $\beta_1 = -1, 0$, and 1 for climbing, en route, and descending, respectively.

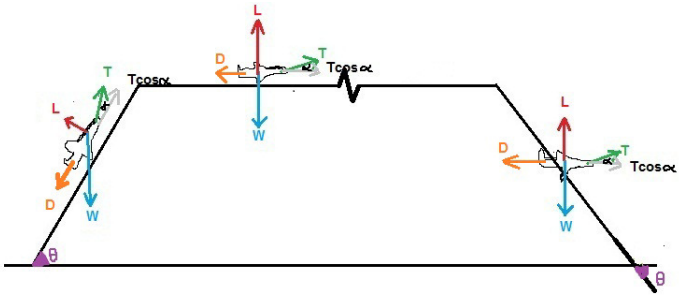

Figure 1: The forces on the aircraft during climbing, en route, and descending. L = lift force, T = thrust force, $W = mg$ = the weight of aircraft, α = the angle of attack, θ = angle between the tip of the aircraft and horizontal, and D = drag force.

In the proposed model, we suppose that the gas outlet of aircraft is not strangled. Therefore, from the flight dynamics formulas [6], we have

$$T_n = \frac{W_a}{g}(v_g - \frac{dx_n}{dt}) \quad \text{and} \quad D_n = \frac{1}{2}\rho_a(\frac{dx_n}{dt})^2 sc_D, \tag{3}$$

where W_a is the weight of the air that enters in the engine, v_g denotes the velocity of output gases, ρ_a is the density of air, s denotes the area of two wings plus the area of aircraft body between them, and the drag coefficient c_D is constant. x_n and g are defined as the same as before.

Although the effects of the headway $\Delta x_n = x_{n+1} - x_n$ and the relative velocity $\Delta v_n = v_{n+1} - v_n$ are not seen on the velocity of air traffic flow, they must be considered in the designing of a flight plan. Therefore, by adding a function F in terms of Δx_n and Δv_n, the equation (2) can be written in the following form

$$m\frac{d^2x_n}{dt^2} = T_n \cos\alpha - D_n + \beta_1 mg \sin\theta B(\Delta x_n, \Delta v_n) + F(\Delta x_n, \Delta v_n). \tag{4}$$

By substituting (3) in (4), we have

$$\begin{aligned}\frac{d^2x_n}{dt^2} = \frac{\gamma}{m}(&\frac{W_a\cos\alpha}{\gamma g}(v_g - \frac{dx_n}{dt}) - (\frac{dx_n}{dt})^2 + \frac{\beta_1 mg\sin\theta B(\Delta x_n, \Delta v_n)}{\gamma} \\ &+ \frac{F(\Delta x_n, \Delta v_n)}{\gamma}),\end{aligned} \tag{5}$$

where $\gamma = \frac{1}{2}\rho_a sc_D$. This equation can be rewritten as follows:

$$\frac{d^2x_n}{dt^2} = a(\frac{W_a\cos\alpha}{\gamma g}(v_g - \frac{dx_n}{dt}) - (\frac{dx_n}{dt})^2 + V(\Delta x_n, \Delta v_n)), \tag{6}$$

where $a = \frac{\gamma}{m}$ and

$$V(\Delta x_n, \Delta v_n) = \frac{\beta_1 mg\sin\theta B(\Delta x_n, \Delta v_n)}{\gamma} + \frac{F(\Delta x_n, \Delta v_n)}{\gamma}. \tag{7}$$

Here a represents the sensitivity of the pilot and $V(\Delta x_n, \Delta v_n)$ (by generalizing the optimal velocity in car-following for air traffic) can be defined as follows:

$$V(\Delta x_n, \Delta v_n) = \frac{v_f - v_{\min}}{2}[\tanh(\Delta x_n - h_c) + \tanh(h_c)] + \frac{\lambda}{a}\Delta v_n, \tag{8}$$

where v_f and $v_{\min}$ are the free and minimal velocity, h_c denotes the safe distance, and the sensitivity λ is defined by

$$\lambda = \eta\frac{[v_n(t + t_d)]^k}{(\Delta x_n)^l}. \tag{9}$$

Here k and l are non-negative parameters, t_d denotes the reaction time, and η is a positive coefficient of proportionality.

From the equations (7) and (8), for $\theta = 0$, we have

$$\begin{aligned}\frac{F(\Delta x_n, \Delta v_n)}{\gamma} &= \frac{v_f - v_{\min}}{2}[\tanh(\Delta x_n - h_c) + \tanh(h_c)] \\ &\quad + \frac{\lambda}{a}\Delta v_n \quad , \end{aligned} \tag{10}$$

For the first term of the right-hand side of equation (7), we suppose that

$$\begin{aligned}\frac{mg\sin\theta B(\Delta x_n, \Delta v_n)}{\gamma} &= V_u(\Delta x_n, \Delta v_n) \\ &= \frac{v_{u,f} - v_{u,\min}}{2}[\tanh(\Delta x_n - h_{u,c}) + \tanh(h_{u,c})] \\ &\quad + \frac{\lambda_u}{a}\Delta v_n\end{aligned}$$

where

$$v_{u,f} - v_{u,\min} = \frac{mg\sin\theta}{\gamma},$$

is the maximum increased speed during climbing, $h_{u,c}$ is the brake distance (it means that the braking begins to work at distance $h_{u,c}$). We define $\lambda_u = \lambda\sigma_u \sin\theta$, where σ_u is a positive constant satisfying $\sigma_u \sin\theta < 1$. A similar analysis can be applied for the descending.

Therefore, from the above discussion, the equation (6) can be written as

$$\frac{d^2x_n}{dt^2} = a[\frac{W_a\cos\alpha}{\gamma g}(v_g - \frac{dx_n}{dt}) - (\frac{dx_n}{dt})^2 + V_s(\Delta x_n)] + \sigma\lambda\Delta v_n, \tag{11}$$

where $V_s(\Delta x_n)$ is given by

$$V_s(\Delta x_n) = \frac{v_f - v_{\min}}{2}[\tanh(\Delta x_n - h_c) + \tanh(h_c)], \quad \sigma = 1,$$

for en route,

$$\begin{aligned}V_s(\Delta x_n) &= \frac{v_f - v_{\min}}{2}[\tanh(\Delta x_n - h_c) + \tanh(h_c)] \\ &\quad - \frac{v_{u,f} - v_{u,\min}}{2}[\tanh(\Delta x_n - h_{u,c}) + \tanh(h_{u,c})], \ \sigma = 1 - \sigma_u\sin\theta,\end{aligned}$$

for climbing, and

$$\begin{aligned}V_s(\Delta x_n) &= \frac{v_f - v_{\min}}{2}[\tanh(\Delta x_n - h_c) + \tanh(h_c)] \\ &\quad + \frac{v_{d,f} - v_{d,\min}}{2}[\tanh(\Delta x_n - h_{d,c}) + \tanh(h_{d,c})] \ , \ \sigma = 1 + \sigma_d\sin\theta,\end{aligned}$$

for descending (see Fig. 1).

By assuming that $h_{u,c} = h_{d,c} = h_c$, these three equations can be written as

$$\begin{aligned} V_s(\Delta x_n) &= \beta(\frac{v_f - v_{\min}}{2}[\tanh(\Delta x_n - h_c) + \tanh(h_c)]) \\ &= \beta V(\Delta x_n). \end{aligned} \tag{12}$$

Here $\beta = 1$ for en route, $\beta = 1 - \beta_0 \sin\theta$ for climbing, and $\beta = 1 + \beta_0 \sin\theta$ for descending, where $\beta_0 = \dfrac{mg}{\gamma(v_f - v_{\min})}$.

3 The macroscopic model

In order to obtain the macroscopic model of (11), we use the method described in [7] and transform the microscopic variables to the macroscopic ones, i.e.,

$$\begin{aligned} &v_n(t) \to v(x,t), \quad v_{n+1}(t) = v(x+\varepsilon, t), \quad \Delta x_n \to \rho(x,t), \\ &V(\Delta x_n(t)) \to v_e(\rho(x,t)), \quad a \to \frac{1}{T_r}, \quad \lambda \to \frac{1}{\tau}, \end{aligned} \tag{13}$$

where $v(x,t)$ and $\rho(x,t)$ are the mean speed and density of flow, respectively, v_e is the equilibrium speed, T_r represents the relaxation time, ε is the distance between the front and the follower aircraft, and τ denotes the reaction time needed by pilots to adjust the speed difference.

Noticing that $v = v(x,t)$, using $\dfrac{d^2x_n}{dt^2} = vv_x + v_t$ and the relation (13) on the microscopic model (11), we have

$$v_t + vv_x = \frac{1}{T_r}(\frac{W_a \cos\alpha}{\gamma g}(v_g - v) - v^2 + \beta v_e) + \frac{\sigma}{\tau}(v(x+\varepsilon, t) - v(x,t)). \tag{14}$$

Expanding the second term of the right-hand side of equation (14) and neglecting higher-order terms, we obtain

$$v_t + vv_x = \frac{1}{T_r}(\frac{W_a \cos\alpha}{\gamma g}(v_g - v) - v^2 + \beta v_e) + \sigma c_0 v_x, \tag{15}$$

where $c_0 = \varepsilon/\tau$.

Therefore, considering the LWR equation (1), the system of the macroscopic model for air traffic flow is as follows:

$$\begin{cases} \rho_t + (\rho v)_x = 0, \\ v_t + (v - \sigma c_0)v_x = \dfrac{1}{T_r}(\dfrac{W_a \cos\alpha}{\gamma g}(v_g - v) - v^2 + \beta v_e), \end{cases} \tag{16}$$

The following initial and boundary values are considered.

$$\begin{aligned} \rho(x,0) &= \rho_0(x), \\ v(x,0) &= v_0(x), \\ \rho(0,t) &= \rho_d, \\ \rho(L,0) &= \rho_u, \\ v(0,t) &= v_0, \\ v(L,0) &= v_n. \end{aligned}$$

It can be easily observed that the characteristic speeds are $\lambda_1 = v, \lambda_2 = v - \sigma c_0$. Since $\sigma c_0 > 0$, the characteristic speeds are not greater than the macroscopic flow speed and the system is hyperbolic.

In order to show the stability of the model, assume that ρ_0 and $v_0 = v_e(\rho_0)$ are the steady-state solutions of equation (16), $\rho = \rho_0 + \xi$ and $v = v_0 + \eta$ are the perturbed solutions of equation (16), where $\xi = \xi(x,t)$ and $\eta = \eta(x,t)$ are small perturbations to the steady-state solutions. As in [7], we can show that how these perturbations evolve over time and the following stability condition is hold:

$$v_0 - \sigma c_0 \leq c \leq v_0,$$

where $c = \frac{d(\rho v)}{d\rho}|_{\rho=\rho_0} = (\rho v)'|_{\rho=\rho_0}$ is the kinematic wave speed.

4 Simulation

As known, in computational physics, upwind schemes denote a class of numerical discretization methods for solving hyperbolic partial differential equations. The Upwind schemes attempt to discretize the hyperbolic partial differential equations by using differencing biased in the direction determined by the sign of the characteristic speeds.

By using the first order upwind scheme [16] for solving the system (16) and noticing that v is positive, we get the difference equations

$$\begin{cases} \rho_i^{j+1} = \rho_i^j + \frac{\Delta t}{\Delta x}\rho_i^j(v_i^j - v_{i+1}^j) + \frac{\Delta t}{\Delta x}v_i^j(\rho_{i-1}^j - \rho_i^j), \\ v_i^{j+1} = v_i^j - \frac{\Delta t}{\Delta x}(v_i^j - \sigma c_0)(v_{i+1}^j - v_i^j) + \frac{\Delta t}{T_r}(\frac{T_i^j \cos\alpha}{\gamma} - (v_i^j)^2 + \beta v_e(\rho_i^j)), \end{cases}$$

for $v_i^j < \sigma c_0$, and

$$\begin{cases} \rho_i^{j+1} = \rho_i^j + \frac{\Delta t}{\Delta x}\rho_i^j(v_i^j - v_{i+1}^j) + \frac{\Delta t}{\Delta x}v_i^j(\rho_{i-1}^j - \rho_i^j), \\ v_i^{j+1} = v_i^j - \frac{\Delta t}{\Delta x}(v_i^j - \sigma c_0)(v_i^j - v_{i-1}^j) + \frac{\Delta t}{T_r}(\frac{T_i^j \cos\alpha}{\gamma} - (v_i^j)^2 + \beta v_e(\rho_i^j)), \end{cases}$$

for $v_i^j \geq \sigma c_0$. Here ρ_i^j, v_i^j and $T_i^j = \frac{W_a}{g}(v_g - v_i^j)$ are respectively density, speed and the thrust force of engine at the grid discrete points. According to Greenshields linear equilibrium speed-density function in [5] and its generalization for air traffic in [14], the equilibrium speed function can be considered as

$$v_e(\rho) = v_{\min} + (v_f - v_{\min})(1 - \frac{\rho}{\rho_{\max}}), \tag{17}$$

where $\rho_{\max}$ denotes the flight occupancy rate as each flight separates with minimal safe distance. The speed v_e approaches to $v_{\min}$ and v_f as ρ approaches to $\rho_{\max}$ and zero, respectively. We recall that

$$\beta = 1 - \beta_0 \sin\theta, \quad \sigma = 1 - \sigma_u \sin\theta,$$

for climbing,

$$\beta = \sigma = 1$$

for en route, and

$$\beta = 1 + \beta_0 \sin\theta, \quad \sigma = 1 + \sigma_d \sin\theta,$$

for descending. Moreover, $c_0 = \frac{\varepsilon}{\tau}$ and $\gamma = \frac{1}{2}\rho_a s c_D$.

The following data are used.

$L = 800$km,
$v_0^j = 240$km/h,
$v_n^j = 220$km/h,
$\theta = 15^o, 0$, and -15^o, for climbing, en route, and descending, respectively,
$\rho_{\max} = 0.125$,
$\Delta t = 1$ minute,
$\Delta x = 16$ km,
$W = mg = 36000$ kg,
$s = 0.000325\ m^2$,
$c_D = 2c_{D_0}$, where $c_{D_0} = 0.02$,
$W_a = 656$ lb/s,
$\beta_0 = 2$,
$T_r = 3$ s,
$v_g = 0.428$ foot/s,
$\sigma_u = \sigma_d = 2$,
$v_f = 900$ km/h,
$v_{\min} = 220$ km/h,
$\alpha = \pi/720 \sim 0.25^o$.

When a flight manager, according to the position of the other planes, investigates a flight plan for one aircraft, he or she wants to prevent shockwaves and rarefaction waves in the density of flow. In a confirmed flight plan, usually, you can see some commands in changing speeds for specified distances. They must be considered in the flight plan to the prevention of the shockwaves and rarefaction waves.

In order to reproduce the evolution of shockwave, rarefaction wave, and small perturbation by the new model, we perform some numerical simulations with the following initial and boundary conditions.

(i) $\rho_d^1 = 0.04, \quad \rho_u^1 = 0.098, \quad \rho^1(x,0) = \begin{cases} 0.04, & 0 \le x \le 380, \\ 0.098, & 380 \le x \le 800, \end{cases}$

(ii) $\rho_d^2 = 0.098\ (\frac{plane}{km}), \quad \rho_u^2 = 0.04\ (\frac{plane}{km}), \quad \rho^2(x,0) = \begin{cases} 0.098, & 0 \le x \le 380, \\ 0.04, & 380 \le x \le 800, \end{cases}$

(iii) $\rho_d^3 = 0.04\ (\frac{plane}{km})$, $\rho_u^3 = 0.04\ (\frac{plane}{km})$, $\rho^3(x,0) = \begin{cases} 0.04, & 0 \le x \le 220, \\ 0.098, & 220 \le x \le 380, \\ 0.04, & 380 \le x \le 800, \end{cases}$

(iv) $\rho_d^4 = 0.098\ (\frac{plane}{km})$, $\rho_u^4 = 0.098\ (\frac{plane}{km})$,

$$\rho^4(x,0) = \begin{cases} 0.098, & 0 \le x \le 220, \\ 0.04, & 220 \le x \le 380, \\ 0.098, & 380 \le x \le 800, \end{cases}$$

(v) $\rho_d^5 = 0.04\ (\frac{plane}{km})$, $\rho_u^5 = 0.04\ (\frac{plane}{km})$,

$$\rho^5(x,0) = \begin{cases} 0.04 + \dfrac{0.098 - 0.04}{220}x, & 0 \le x \le 220, \\ 0.098, & 220 \le x \le 380, \\ 0.098 + \dfrac{0.04 - 0.098}{800 - 380}(x - 380), & 380 \le x \le 800. \end{cases}$$

Here ρ_d^i, ρ_u^i $(1 \le i \le 5)$ denote the downstream and upstream densities. For these cases, the above initial densities ($\rho^j(x,0)$ for $1 \le j \le 5$) have been displayed in Figures 2-6. The initial speeds are derived by $v = v_e(\rho)$. If the computed value v_i^{j+1} does not satisfy $v_{\min} \le v_i^{j+1} \le v_f$, we obtain v_i^{j+1} by (17).

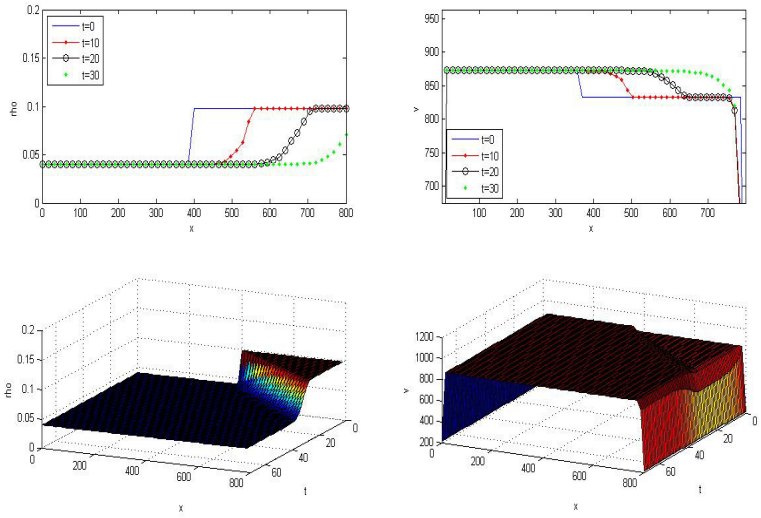

Figure 2: Evolution of density and speed in different positions for case (i) **above:** at times $t = 0$, $t = 10$, $t = 20$, and $t = 30$; **bottom:** during the next 70 minutes.

In Figures 2-6, two above figures show the evolution of density and speed for initial and boundary conditions (i) to (v) at times $t = 0$, $t = 10$, $t = 20$, and $t = 30$ minutes. Moreover, two bottom figures display the evolution in the next 70 minutes.

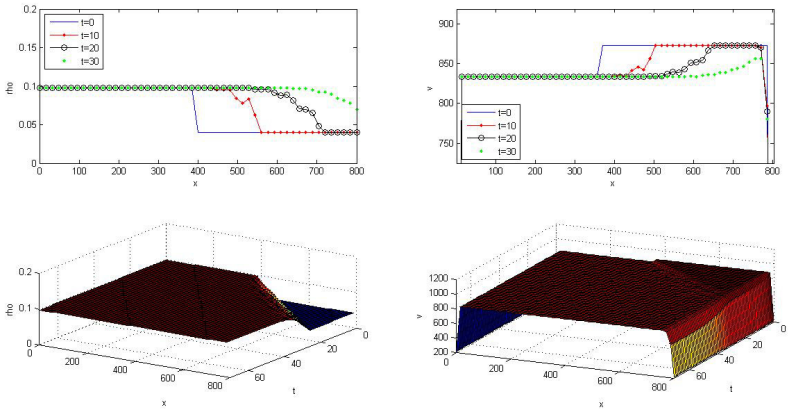

Figure 3: Evolution of density and speed in different positions for case (ii) **above:** at times $t = 0$, $t = 10$, $t = 20$, and $t = 30$; **buttom:** during the next 70 minutes

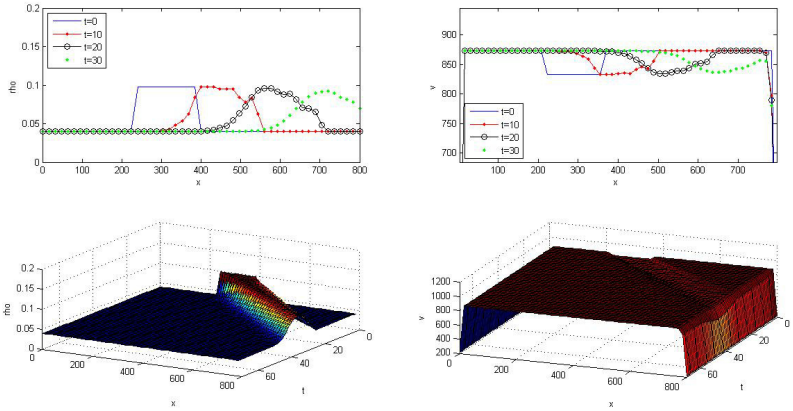

Figure 4: Evolution of density and speed in different positions for case (iii) **above:** at times $t = 0$, $t = 10$, $t = 20$, and $t = 30$; **bottom:** during the next 70 minutes.

Noticing the above Figures, the predicted results for the next 70 minutes, under the two Riemann initial conditions, are obtained. These results are consistent with choosing the equilibrium speed v_e in the model. The relation (17) shows a linear velocity-density relation in which v and ρ are changing in opposite directions.

In all of the above Figures, the density is less than the maximum during the airway. The positions where the density is not smaller than the maximum, are marked with red stars. This means that in those positions the safe distance is

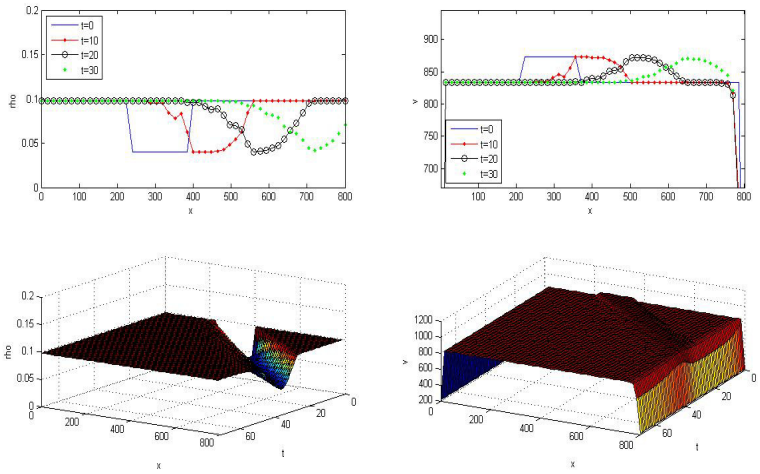

Figure 5: Evolution of density and speed in different positions for case (iv) **above:** at times $t = 0$, $t = 10$, $t = 20$, and $t = 30$; **bottom:** during the next 70 minutes.

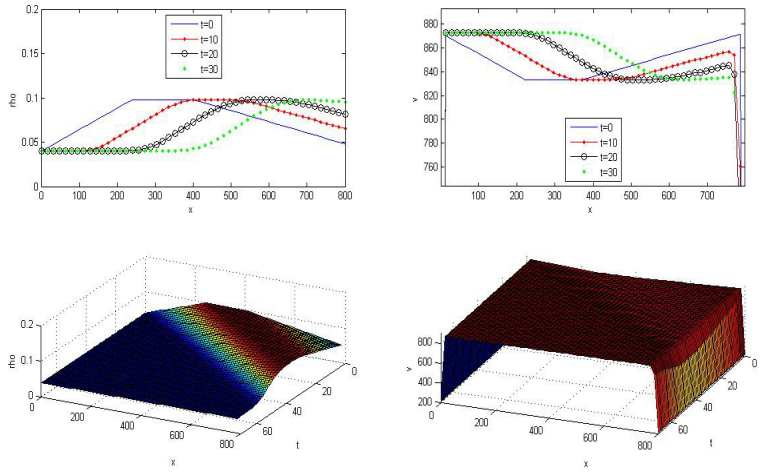

Figure 6: Evolution of density and speed in different positions for case (v) **above:** at times $t = 0$, $t = 10$, $t = 20$, and $t = 30$; **bottom:** during the next 70 minutes.

not met. Therefore, the flight plan that leads to this situation must be changed. Figures 7, 8, and 9 show such a situation for some initial boundary value problems that are induced by some given flight plans.

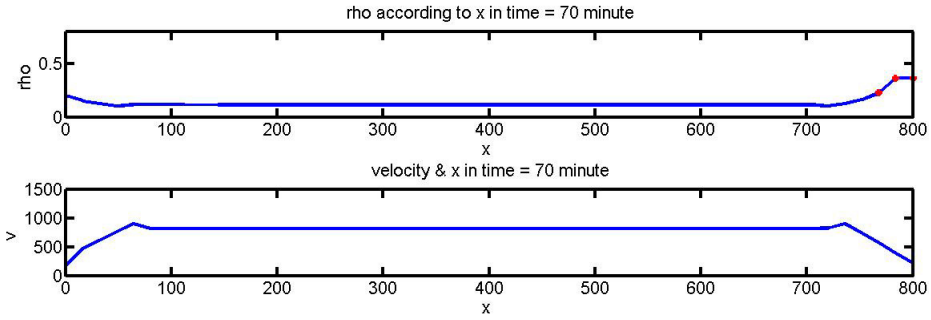

Figure 7: Density at the end of airway is more than Max.

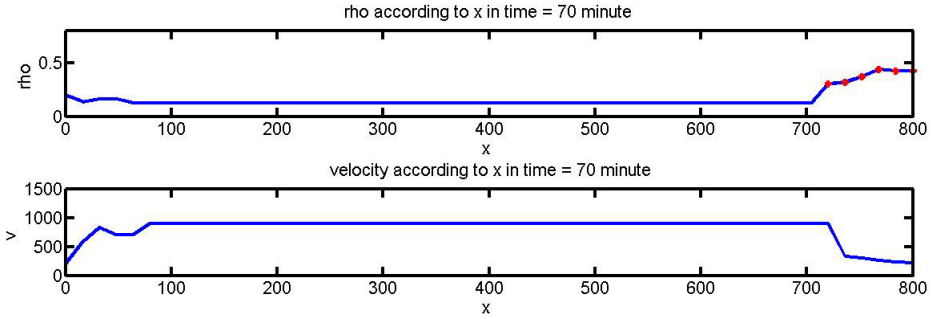

Figure 8: Density at the end of airway is more than Max.

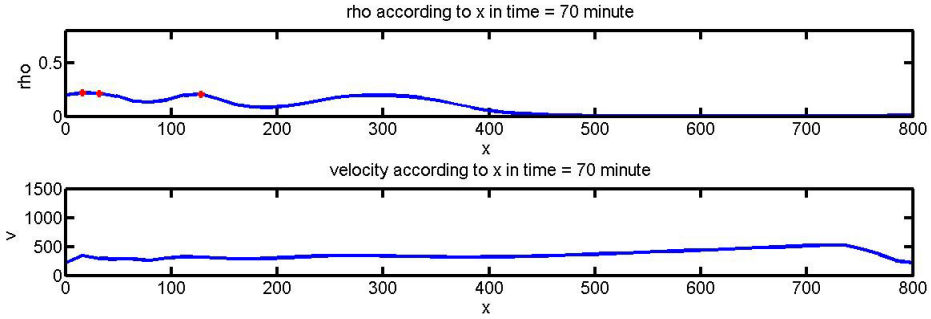

Figure 9: Density in some positions is more than Max.

5 Conclusion

In this paper, we have proposed a new macroscopic nonlinear second-order model for air traffic flow. We have considered the changes in density and speed of flow for a monolayer and single-direction airway. By extending the car-following theory for air traffic flow, we have obtained the macroscopic form of the model. It is shown that, in the proposed model, the characteristic speeds are not greater than the macroscopic flow velocity. The upwind differencing scheme has been used to discrete the proposed model.

By choosing a linear density-velocity function for the equilibrium speed v_e, the results of simulations confirm this relation between velocity and density. Moreover, numerical results show that the proposed model can reproduce the evolution of shockwave, rarefaction wave, and small perturbation. They also can be applied for predicting the density of flow during airway. By them, if the density of flow is more than the maximum in some positions, the flight plan will not be confirmed and must be changed.

References

[1] A.M. Bayen, P. Grieder, G. Meyer and C.J. Tomlin, *Lagrangian delay predictive model for sector-based air traffic flow*, J. Guid. Control Dyn. **28**(5) (2005).

[2] A. M. Bayen, R. L. Raffard and C. J. Tomlin, *Eulerian network model of air traffic flow in congested areas*, Proceedings of the American Control Conference, Boston, (2004) 5520-5526.

[3] A. M. Bayen, R. L. Raffard and C. J. Tomlin, *Adjoint-based control of a new Eulerian network model of air traffic flow*, IEEE Trans. Control Syst. Tech. **14**(5) (2006).

[4] D. Chen, M. Hu, Y. Ma and J. Yin, *A network-based dynamic air traffic flow model for short-term en route traffic prediction*, J. Adv. Transport. **50** (2016) 2174-2192.

[5] B. D. Greenshields, *A study in highway capacity*, Highway Research Board Proceedings, **14** (1935) 448-477.

[6] H. Hu, W. Shyy and T. I-P. Shih, *Lift, thrust and flight*, Encyclopedia of Aerospace Engineering, John Wiley and Sons, 2010.

[7] R. Jiang, Q.S. Wu and Z.J. Zhu, *A new continuum model for traffic flow and numerical tests*, Transport. Research B **36** (2002) 405-419.

[8] Q. Ma, Y. Wan and D. Sun, *Probabilistic collocation method in solving Eulerian model for air traffic flow management*, Garden Grove, CA, June 19-21, 2012.

[9] P.K. Menon, G. D. Sweriduk and K.D. Bilimoria, *New approach for modelling, analysis, and control of air traffic flow*, J. Guid. Control Dyn. **27**(5) (2004) 737-744.

[10] P.K. Menon, G.D. Sweriduk and K.D. Bilimoria, *Air traffic flow modeling, analysis and control*, in Proceedings of the AIAA Guidance, Navigation, and Control Conference and Exhibit, (2003) 11-14.

[11] P.K. Menon, G.D. Sweriduk, T. Lam, G.M. Diaz and K.D. Bilimoria, *Computer-Aided Eulerian air traffic flow modelling and predictive control*, J. Guid. Control Dyn. **29**(1) (2006) 12-19.

[12] I.S. Strub and A. M. Bayen, *Optimal control of air traffic networks using continuous flow models*, AIAA Conference on Guidance, Control and Dynamics, (2006) 2006-6228.

[13] D. Sun, I. Strub and A.M. Bayen, *Comparison of the performance of four Eulerian network flow models for strategic air traffic management*, Netw. Heterog. Media **2**(4) (2007) 569-595.

[14] S. Wang, *Area air traffic flow optimal scheduling under uncertain weather*, International Conference on Computational Intelligence and software Engineering, 2009.

[15] L. Wang, X. Zhang, and Z. Zhang, *Following phenomenon and air freeway flow model*, J. Southwest Jiaotong Univ. **47**(1) (2012) 158-162.

[16] H.C. Yee, *Upwind and symmetric shock-capturing schemes*, Ames Research Center, Moffett Field, California , 1987.